Pergamon

Geochimica et Cosmochimica Acta, Vol. 63, No. 7/8, pp. 1173–1180, 1999

0016-7037/99 $20.00 + .00

PII S0016-7037(99)00289-0

The relative effects of pressure, temperature and oxygen fugacity on the solubility of sulfide in mafic magmas

JOHN A. MAVROGENES*[1,2] and HUGH ST.C. O'NEILL[1]

[1]Research School of Earth Sciences, The Australian National University, Canberra, 0200, Australia
[2]Geology Department, Australian National University, Canberra, 0200, Australia

(*Received June* 11, 1997; *accepted in revised form September* 9, 1998)

Abstract—The sulfur contents at sulfide saturation (SCSS) of a basaltic and a picritic melt have been measured experimentally as a function of pressure and temperature from 5 to 90 kb and 1400–1800°C, using piston-cylinder and multi-anvil solid media pressure devices. Three distinct regimes of oxygen fugacity were investigated, imposed by the use of Fe_{100}, $Fe_{40}Ir_{60}$, and $Fe_{20}Ir_{80}$ capsules. The compositions of quenched run products, including the S contents of the silicate glasses, were determined by electron microprobe analysis. Theoretical considerations suggest that SCSS values (in ppm) can be described by an equation of the form:

$$\ln[S/ppm]_{SCSS} = \frac{A}{T} + B + \frac{CP}{T} + \ln a_{FeS}^{sulfide}$$

where A and B are functions of the composition of the silicate melt. This equation implies that SCSS is independent of fO_2 and fS_2, except insofar as these factors influence the nature of the sulfide liquid (hence $a_{FeS}^{sulfide}$). The experiments reported here confirm this. The SCSS of both the basaltic and picritic compositions are rather insensitive to temperature, but show a strong exponential decrease with increasing pressure. Consequently, a magma generated in equilibrium with residual sulfide in the mantle becomes under saturated in sulfide during adiabatic ascent. At low pressure, sulfide saturation should occur only after substantial crystallization, under closed-system conditions, or after significant modification via assimilation (e.g., of S-rich sediments).

1. INTRODUCTION

The solubility of sulfur in silicate melts bears on a wide range of processes, including magmatic sulfide deposition, trace-element behavior, sulfur degassing from volcanic eruptions (hence global climate change), and possibly core/mantle differentiation. Although there is extensive information on many aspects of sulfide solubilities in silicate slags in the metallurgical literature, this information is generally on silicate compositions far removed from natural melts, and pertains only indirectly to the central question of interest to geologists, that is; "What is the amount of sulfur dissolved in a silicate melt saturated with an immiscible molten sulfide phase?"—in other words, the sulfur content at sulfide saturation, or SCSS (Shima and Naldrett, 1975). Moreover, the metallurgical studies cover only a limited range of temperature (Sosinsky and Somerville, 1986), and do not consider the geologically important variable of pressure. Our current knowledge of the effect of pressure on SCSS may be summarized by the following quotation from Wallace and Carmichael (1992): "The experimental data on the effect of pressure are equivocal, with some studies showing an increase in S solubility and others a decrease or no measurable effect (Wendlandt, 1982; Carroll and Rutherford, 1985; Naldrett, 1989; Luhr, 1990)". The confusion regarding the affects of pressure on sulfide (S^{2-}) solubilities is illustrated in Fig. 1.

For economic geologists, it is important to know the effect of pressure on sulfur solubilities, to determine, firstly, whether a melt originating in the mantle is sulfide saturated at source and, secondly, whether after adiabatic ascent the melt arrives at the surface sulfide saturated. Given the mantle's likely sulfur content of ~200 ppm S in the primitive mantle, and ~150 ppm in the depleted (MORB source) mantle (Lorand, 1990, O'Neill, 1991), and the relatively low degrees of partial melting for basaltic and picritic melts, it is likely that they leave their source sulfide saturated (i.e. in equilibrium with residual sulfide). Furthermore, if SCSS decreases strongly with increasing pressure as reported by Wendlandt (1982), then "basaltic" melts will arrive at the surface sulfide under-saturated, and the precipitation of magmatic sulfide deposits would require extensive modification via fractional crystallization or assimilation.

1.1. Theoretical Considerations

Fincham and Richardson (1954) proposed that at moderate to low oxygen fugacities (i.e., fO_2 more reducing than that defined by the quartz-fayalite-magnetite [QFM] equilibrium), sulfur dissolves in silicate melts as S^{2-}, and does so by replacing O^{2-} on the anion sublattice, as described by the reaction:

$$O^{2-} + \tfrac{1}{2}S_2 = S^{2-} + \tfrac{1}{2}O_2 \quad (1)$$

Because in silicate melts the number of O^{2-} anions greatly exceeds the number of all other anions including S^{2-}, the activity of O^{2-} is assumed to be constant. Reaction 1 therefore suggests the relationship:

$$C_S = \left[S/ppm \left(\frac{fO_2}{fS_2} \right)^{\frac{1}{2}} \right] \quad (2)$$

*Author to whom correspondence should be addressed (John.Mavrogenes@anu.edu.au).

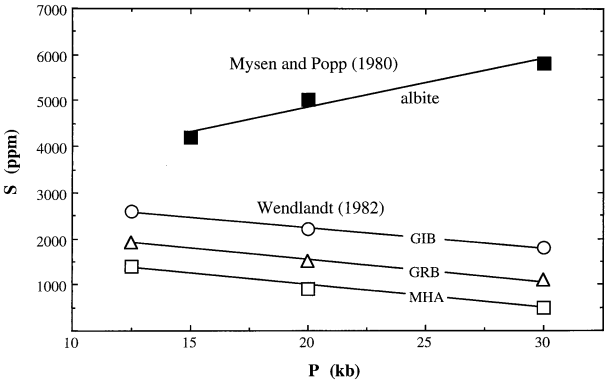

Fig. 1. Contrasting sulfur solubility vs. pressure trends for experiments reported by Mysen and Popp (1980) and by Wendlandt (1982) on Goose Island Basalt (GIB), Grand Ronde Basalt (GRB), and Mt. Hood Andesite (MHA).

where C_S, the "sulfide capacity" of the melt, may be thought of as an equilibrium constant for Reaction 1, and is therefore a function of melt composition, temperature and pressure. Fincham and Richardson (1954) experimentally verified this relationship by holding metallurgical slag compositions constant while varying fO_2 and fS_2 independently at 1 atm. An extensive body of subsequent work reported in the metallurgical literature has repeatedly confirmed this finding for a wide compositional range of metallurgical slags (for a summary of this literature, see review by Young et al., 1992), and recently we have also verified this relationship for a wide variety of basaltic and haplobasaltic melt compositions at atmospheric pressure using similar experimental methodology (Mavrogenes and O'Neill, in preparation). At higher oxygen fugacities (fO_2 > QFM), sulfur dissolves in silicate melts predominantly as the sulfate species (SO_4^{2-}). In what follows we confine our attention to the low fO_2 regime, which is appropriate for most basaltic magmas.

The equilibrium between a silicate melt and a sulfide phase can be described by the reaction:

$$\underset{\text{silicate melt}}{\text{FeO}} + \tfrac{1}{2}S_2 = \underset{\text{sulfide}}{\text{FeS}} + \tfrac{1}{2}O_2 \qquad (3)$$

for which:

$$-\Delta G°(3)/RT = \ln a_{FeS}^{sulfide} - \ln a_{FeO}^{silicate} + \ln \left(\frac{fO_2}{fS_2}\right)^{\frac{1}{2}} \qquad (4)$$

substituting Eqn. 2 into Eqn. 4 and to eliminate

$$\left(\frac{fO_2}{fS_2}\right)^{\frac{1}{2}}$$

we obtain:

$$\ln [S/ppm]_{SCSS} = \Delta G(3)/RT + \ln C_S - \ln a_{FeS}^{sulfide} + \ln a_{FeO}^{sulicate} \qquad (5)$$

The sulfide capacity C_S can be considered to comprise the sum of a number of equilibrium constants, K_{MS}, each of which describes a reaction of the type:

$$M_xO + \tfrac{1}{2}S_2 = M_xS + \tfrac{1}{2}O_2 \qquad (6)$$

where $M = Fe^{2+}$, Ca, Mg, Na, K, Ti, etc. The deconvolution of C_S into its component values of K_{MS} need not concern us here. It suffices to assume that the relationship between C_S and temperature and pressure is described by analogy with the usual relationship between an equilibrium constant and these variables, that is:

$$\ln C_S = -\frac{\Delta H_{Cs}}{RT} + \frac{\Delta S_{Cs}}{R} - \frac{P\Delta V_{Cs}}{RT} \qquad (7)$$

where ΔH_{Cs}, ΔS_{Cs}, and ΔV_{Cs} are mean values of enthalpy, entropy and molar volume, assumed to be constant over the range of temperature and pressure considered here. This relationship is commonly assumed in the metallurgical literature (Sosinsky and Sommerville, 1986), albeit without the ΔV_{Cs} term, because the metallurgical literature is not concerned with the effect of geological pressures. The available data (summarized in Sosinsky and Sommerville, 1986) indicates that both ΔH_{Cs} and ΔS_{Cs}, vary with the major-element composition of the silicate melt.

The quantities $\Delta G°(3)/RT$ and $\ln a_{FeS}^{silicate}$ may also be split into temperature- and pressure-dependent enthalpy, entropy and volume terms in the usual way:

$$\frac{\Delta G°(3)}{RT} = \frac{\Delta H°(3)}{RT} - \frac{\Delta S°(3)}{R} + \frac{P\Delta V°(3)}{RT} \qquad (8)$$

$$\ln a_{FeO}^{silicate} = \frac{\Delta \bar{H}°_{FeO}}{RT} - \frac{\Delta \bar{S}°_{FeO}}{R} + \frac{\Delta \bar{V}°_{FeO}}{RT} \qquad (9)$$

Combining these equations into Eqn. 5, we obtain the form expected for the SCSS as a function of pressure and temperature:

$$\ln[S/ppm]_{SCSS} = \frac{A}{T} + B + \frac{CP}{T} + \ln a_{FeS}^{sulfide} \qquad (10)$$

where

$$A = (-\Delta H_{Cs} + \Delta H°(3) + \Delta \bar{H}°_{FeO})/R$$

and so forth. A, B and C are constants for a given silicate melt composition, and may be determined by experiment.

An important feature of Eqn. 10 that deserves further comment, because it may seem somewhat counterintuitive, is that although the position of the sulfide saturation surface in T-P-composition space depends on both fS_2 and fO_2 (as expressed in Eqn. 4), the actual value of the SCSS in a silicate magma of fixed composition is independent of fS_2 and fO_2, except in so far as these quantities affect the composition of the sulfide liquid and hence $a_{FeS}^{sulfide}$. This is empirically confirmed by the experimental results in this study (see below). Compositional changes, such as increased FeO in the silicate melt (as demonstrated by Haughton et al., 1974) strongly affect SCSS because the resultant increase in Cs greatly overwhelms the negative effects of $a_{FeO}^{silicate}$in Eqn. 5.

Under most geologically relevant T-P-fO_2-fS_2 conditions the composition of the sulfide liquid in the system Fe-S-O in equilibrium with basic magmas is close to FeS stoichiometry, with little or no excess O or Fe, and hence $a_{FeS}^{sulfide} \approx 1$. Although a few percent of oxygen can dissolve in FeS-rich sulfide melts at 1 bar (Kress, 1997), the solubility of O in

Table 1. Compositions of starting glasses and silicate run products.

	SiO_2	TiO_2	Al_2O_3	FeO(t)	MgO	CaO	Na_2O	K_2O	Total
Starting Material									
Basalt	48.80	2.00	17.70	10.50	6.95	10.05	2.90	1.10	100.00
Picrite	46.50	2.00	12.60	10.10	17.20	9.70	1.65	0.20	100.00
Run Products									
Basalt									
MAV1	47.72	1.59	17.22	13.12	7.01	9.09	2.89	1.21	99.85
MAV14	49.08	1.69	17.66	11.20	7.05	10.01	2.89	0.92	100.5
MAV2	47.95	1.57	17.32	13.01	7.13	8.60	3.00	1.20	99.78
MAV4	48.85	1.66	17.54	10.94	7.23	9.27	3.04	1.25	99.77
MAV9	48.84	1.61	16.88	13.31	6.96	9.57	2.99	0.89	101.05
MAV10	54.75	1.33	15.15	10.53	5.73	7.74	3.00	0.67	98.88
MAV5	47.92	1.50	16.58	14.17	6.32	8.79	3.25	1.32	99.83
MAV8	49.10	1.60	17.13	12.29	6.99	9.62	2.98	0.88	100.58
MAV12	51.91	2.02	18.95	8.27	5.72	9.21	2.96	1.27	100.32
MAV6	51.98	1.59	14.21	11.56	6.54	10.07	3.71	0.81	100.46
MAV7	51.65	1.79	16.00	10.65	5.78	8.86	3.59	1.19	99.51
MAV65	52.00	2.13	17.68	8.40	7.30	10.18	1.34	0.97	100.00
MAV64	51.80	2.50	17.70	8.60	7.30	9.94	1.22	0.90	99.96
MAV27	50.42	1.80	16.92	9.95	7.06	9.66	2.45	0.79	99.05
MACV26	47.62	1.76	17.88	10.17	6.73	9.52	2.71	0.85	97.23
MAV32	50.79	1.81	16.50	8.68	6.84	8.86	2.10	0.68	96.26
MAV29	51.34	1.57	17.62	9.80	7.44	9.29	2.93	0.80	100.76
MAV31	49.55	0.67	17.21	8.16	7.76	10.55	2.64	0.72	97.26
MAV54	50.22	1.72	17.07	10.71	7.25	9.33	2.64	0.80	99.74
MAV55	50.58	1.71	17.04	10.88	7.56	9.16	2.92	0.75	100.59
MAV45	49.35	1.66	16.60	6.27	10.39	10.68	2.23	0.60	97.77
MAV68	50.91	1.65	17.23	9.31	7.58	10.15	2.09	0.56	99.49
MAV69	50.20	1.60	17.21	10.22	7.40	10.11	1.90	0.90	99.54
Picrite									
MAV34	47.66	1.77	10.74	12.20	16.87	8.51	1.79	0.34	99.87
MAV36	47.34	1.78	9.48	15.56	15.68	8.45	1.50	0.33	100.13
MAV42	48.55	1.64	10.47	11.47	17.01	8.35	1.51	0.34	99.35
MAV58A	47.07	0.90	9.92	15.49	15.18	8.83	1.89	0.37	99.65
MAV52	48.88	0.71	10.54	11.57	16.31	9.76	1.71	0.39	99.87

Compositions of silicate glass starting material.

sulfide melts seems to decrease rapidly with increasing pressure, consistent with a large partial molar volume of FeO in FeS melts, which may be independently deduced from the density measurements of Kaiura and Toguri (1979). Thus no O could be detected in the quenched sulfide in this study, see below. A similar lack of detectable oxygen in the quenched sulfide of his experimental run products was noted, and discussed, by Wendlandt (1982).

The presence of significant Ni, which partitions heavily into the sulfide phase, in primary terrestrial magmas is a complication not considered here, but which warrants further study.

1.2. Experimental Design

Standard piston-cylinder techniques were used for experiments in the range 5–55 kb. The experiments performed at 1400 and 1500°C were carried out in talc-pyrex assemblies, using the "piston-in" method with a ~10% correction for friction. Experiments at 1800°C used MgO sleeves and inserts and W-Re thermocouples (Ohtani and Ringwood, 1984). The experiment at 55 kb used a CaF_2 sleeve, and a 6% pressure correction. One MA-8 multi-anvil experiment was performed at 1800°C and 90 kb (Ringwood and Hibberson, 1990).

Starting materials consisting of powdered glasses of a basaltic and a picritic composition (Table 1), plus 2% synthetic FeS were loaded into capsules made of Fe, $Fe_{40}Ir_{60}$ or $Fe_{20}Ir_{80}$ (atomic proportions) alloy, and sealed with tight-fitting lids of the same metal composition. These compositions were chosen because more mafic melts (MgO > 18%) do not quench to a homogenous silicate glass, making electron microprobe analyses of dissolved sulfur difficult at best. All oxide mixes were carefully dried before use, and run products were spot checked for the presence of water by FTIR to ensure that they were anhydrous. The manufacture of the Fe-Ir capsules, and the principles behind their use, will be described elsewhere (O'Neill and Mavrogenes, submitted). Because the masses of the capsules are large compared to the masses of the charges (typical Fe-Ir capsules used here weighed 0.15 to 0.20 g and contained charges weighing 0.015 to 0.020 g: thus the ratio of capsule to charge is about 10:1 by weight), the iron and iron-bearing alloy capsules buffer oxygen fugacity (fO_2) via the reaction:

$$\underset{\text{silicate}}{2\,FeO} = \underset{\text{metal}}{2\,Fe} + O_2 \qquad (11)$$

From which oxygen fugacity may be calculated:

$$\log fO_2 = -\Delta G^{o}_{(11)}/22.3RT + 2\log a^{\text{silicate}}_{FeO} - 2\log a^{\text{metal}}_{Fe} \qquad (12)$$

Activity-composition relations of FeO in silicate melts are discussed in Holzheid et al. (1997). Activity-composition rela-

Table 2. Run conditions and summary of experimental results.

	Time (h)	Capsule	log fO_2^* (ΔIW)	P (kb)	T (°C)	S (ppm)	Obs. St. Dev.	S_{calc} (ppm)	X_{FeS}	a_{FeS} (1 atm)
Basalt										
MAV1	4	Fe_{100}	−1.56	5	1400	1120	65	820	ND	0.50
MAV14	4	Fe_{100}	−1.69	10	1400	630	35	700	ND	0.50
MAV2	4	Fe_{100}	−1.55	15	1400	590	40	620	ND	0.50
MAV4	18	Fe_{100}	−1.70	15	1400	420	20	575	ND	0.50
MAV9	4	Fe_{100}	−1.54	15	1400	840	95	610	0.35	0.50
MAV10	4	Fe_{100}	−1.72	15	1400	395	20	570	ND	0.50
MAV5	4	Fe_{100}	−1.47	25	1400	525	70	480	ND	0.50
MAV8	4	Fe_{100}	−1.61	25	1400	290	30	430	ND	0.50
MAV12	18	Fe_{100}	−1.95	25	1400	350	60	460	0.27	0.50
MAV6	4	Fe_{100}	−1.66	35	1400	230	110	340	ND	0.50
MAV7	4	Fe_{100}	−1.72	35	1400	220	120	335	ND	0.50
MAV65	4	$Fe_{40}Ir_{60}$	+0.22	5	1400	1640	80	1630	1.0	1.0
MAV64	4	$Fe_{40}Ir_{60}$	+0.23	15	1400	1220	65	1250	1.0	1.0
MAV27	4	$Fe_{20}Ir_{80}$	+1.85	5	1400	1725	60	1635	1.0	1.0
MAV26	4	$Fe_{20}Ir_{80}$	+1.85	15	1400	1380	100	1250	1.0	1.0
MAV32	4	$Fe_{20}Ir_{80}$	+1.52	5	1500	1800	180	2030	1.0	1.0
MAV29	4	$Fe_{20}Ir_{80}$	+1.55	15	1500	1570	75	1600	1.0	1.0
MAV31	4	$Fe_{20}Ir_{80}$	+1.39	25	1500	880	130	1180	1.0	1.0
MAV54	4	$Fe_{20}Ir_{80}$	+1.10	5	1800	2955	360	3480	1.0	1.0
MAV55	4	$Fe_{20}Ir_{80}$	+1.02	40	1800	1855	80	1770	1.0	1.0
MAV45	0.17	$Fe_{20}Ir_{80}$	+0.43	90	1800	615	20	600	1.0	1.0
MAV68	4	$Fe_{40}Ir_{60}$	+0.37	35	1800	1875	220	1900	1.0	1.0
MAV69	4	$Fe_{40}Ir_{60}$	+0.31	55	1800	1335	65	1280	1.0	1.0
Picrite										
MAV34	4	$Fe_{20}Ir_{80}$	+1.76	5	1500	4010	645	3760	1.0	1.0
MAV36	4	$Fe_{20}Ir_{80}$	+1.95	15	1500	3125	250	2940	1.0	1.0
MAV42	4	$Fe_{20}Ir_{80}$	+1.69	15	1500	2750	185	2930	1.0	1.0
MAV58A	4	$Fe_{20}Ir_{80}$	+1.40	10	1800	3370	580	3260	1.0	1.0
MAV52	4	$Fe_{20}Ir_{80}$	+1.06	40	1800	1650	310	1720	1.0	1.0

* Calculated using thermodynamic data from Woodland and O'Neill (1977), with $a_{FeO} = 1.7\ X_{FeO}$ from Holzheid et al. (1997). Experimental results, including: sample number: silicate composition (comp.), bas = basalt, pic = picrite; capsule type (Fe = $Fe_{100}Ir_0$, $Fe_{40}Ir_{60}$, and Fe20 = $Fe_{20}Ir_{20}$ alloy); pressure (P) in kilobars; temperature (T) in degrees centigrade; average sulfur content (in ppm); standard deviation (SD) of sulfur analyses; Scale = calculated S from regression fit [eqn 10, Table 3]; X_{FeS} = composition of sulfide phase; a_{FeS} estimated relative to pure FeS.

tions in Fe-Ir alloys are reviewed in Woodland and O'Neill (1997).

For melts with $a_{FeO}^{sil\ melt} \sim 0.1$ (as used here), the pure Fe capsules buffer the oxygen fugacity at about two log units below the "Fe-FeO" (iron-wüstite or IW) equilibrium, whereas at 1400°C the $Fe_{40}Ir_{60}$ capsules impose an oxygen fugacity half a log-bar unit above IW, and the $Fe_{20}Ir_{80}$ capsules an oxygen fugacity two log-bar units above IW, or about one log unit below the (extrapolated) position of the quartz-fayalite-magnetite equilibria. This last oxygen fugacity is typical of much of the upper mantle, as deduced from olivine-orthopyroxene-spinel oxygen barometry (O'Neill and Wall, 1987). Values of oxygen fugacity in each experiment, calculated from Eqn. 12, are given in Table 2.

In addition to controlling fO_2, an advantage of using Fe-Ir capsules is the high melting point of Ir-rich alloy, that permits experimentation to much higher temperatures than would be possible using pure Fe capsules. The solubility of Ir in the molten FeS under the conditions of our experiments seems to be extremely low ($\leq$500 ppm Ir).

Major elements and sulfur were analyzed on the Cameca Microbeam electron probe at the Research School of Earth Sciences, ANU. WDS analyses of sulfur in silicate glass utilized a PET crystal, 15 kV accelerating voltage and 40 nA sample current and a counting time of 2 min. A troilite standard was used for calibration, and peak positions on the sample were maximized relative to troilite. The limit of detection for S was 60–70 ppm. All runs quenched to a homogenous silicate glass containing blebs of immiscible sulfide. The main difficulty encountered during electron microprobe analysis was the avoidance of small blebs of sulfide in the silicate glass, particularly when these occured below the polished surface of the glass, and thus were not apparent in back-scattered electron images. The results (Tables 1 and 2) represent means and standard deviations of twelve analyses of each sample.

Diffusion rates of S^{2-} in silicate melts are $\sim 10^{-12}$ $m^2 s^{-1}$ at 1400°C (Watson, 1994), indicating that diffusive equilibration of S in the experiments is expected to occur over 100 μm distances in $\sim$3 h at this temperature. Accordingly, run durations at 1400°C were 4 h or longer (Table 2). Similar run durations were used by Wendlandt (1982). The attainment of equilibrium in the experiments is indicated by the homogenous distribution of S in the quenched glasses, and by the lack of any apparent time-dependence in the results, for example, for those experiments run at different times (Table 2).

2. RESULTS

The immiscible sulfide phase in runs performed in both compositions of FeIr capsules was stoichiometric FeS in com-

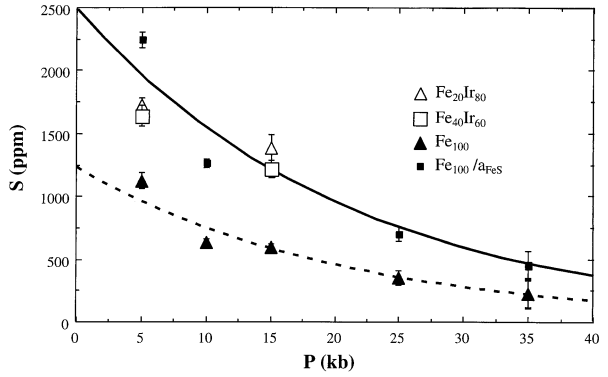

Fig. 2. SCSS in synthetic basalt at 1400°C vs. pressure. The dashed curve is an exponential fit to results of experiments in Fe_{100} capsules (solid symbols). The solid curve is fit to the same results crudely corrected for dilution by Fe (S/a_{Fes}). Note that experiments carried out in $Fe_{60}Ir_{40}$ and $Fe_{80}Ir_{20}$ capsules (open symbols) fit closely to the solid curve despite the different fO_2 imposed by the capsules (see Table 2). Error bars represent observed 2σ errors on analyses.

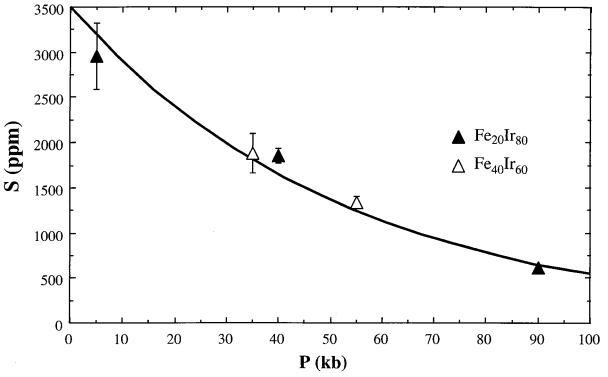

Fig. 3. SCSS in synthetic basalt at 1800°C vs. pressure. Experiments in $Fe_{20}Ir_{80}$ capsules (solid symbols) fit the same exponential function as those in $Fe_{40}Ir_{60}$ capsules (open symbols) despite the different fO_2 imposed by the capsules (see Table 2). Error bars represent observed 2σ errors on analysis.

position, and quenched to nearly pure single phase troilite (Ir $\leq$ 500 ppm). We were unable to distinguish any oxide associated with this sulfide, indicating that the oxygen content of the original sulfide liquid was low. The immiscible sulfide liquids in runs performed in the Fe capsules quench to a mixture of troilite (FeS) and Fe metal. The original (pre-quench) sulfide melts in these runs are constrained to lie along the Fe metal saturation surface of the Fe-FeS phase diagram, at the appropriate pressure. Image analysis of back-scattered-electron SEM images enabled the phase proportions and the original pre-quench composition to be estimated in a two runs (Table 2).

To compare the results obtained for SCSS in the Fe capsules ($a_{FeS} < 1$) with those in the Fe-Ir capsules ($a_{FeS} = 1$), it is necessary to calculate the appropriate value of a_{FeS}. We have used the thermodynamic model for liquids in the Fe-S system at 1 bar of Kongoli et al. (1998) to calculate the value of a_{FeS} to be 0.50 at Fe-saturation at 1400°C, relative to a standard state of pure liquid FeS. An identical result is achieved using the model of Chuang et al. (1985). It is not yet possible, however, to extend such a calculation to high pressures. Based not only on our observations, but also on the earlier, more extensive work of Brett and Bell (1969) and Usselman (1975), it is apparent that the shape of the Fe saturation surface in the Fe-S phase diagram changes dramatically with pressure in the pressure regime of interest to this study, indicating large changes in the structure and properties of Fe-FeS melts. We have therefore perforce used this estimate of $a_{FeS} = 0.50$ at all pressures.

Experimental results are tabulated in Table 2. Series of isothermal experiments are plotted as a function of pressure in Fig. 2 (1400°C) and Fig. 3 (1800°C). Note that results at both temperatures fit well to exponential functions. In Fig. 2 results from experiments carried out in Fe capsules are plotted as raw data, and, as discussed above, as "corrected" values S_{corr} ($S_{corr} = S/a_{Fes}$) for direct comparison with experiments carried out in FeIr capsules (where $a_{FeS} = 1$). At 1400°C runs carried out under three different fO_2 (Table 2) fit the same function within the considerable uncertainties of our "correction" (Fig. 2). At 1800°C runs buffered at two different fO_2 (Table 2) show unequivocally that SCSS is insensitive to changes in fO_2 (Fig. 3).

The measured values of SCSS were fitted to an equation with the form of Eqn. 10 by multiple non-linear least squares regression. Data were weighted assuming uncertainties (one standard deviation) of 10°C in temperature for runs at 1400°C and 1500°C, or 30°C at 1800°C, 3% in pressure, 0.02 in a_{FeS} for the runs in pure Fe capsules (for runs in FeIr capsules, we used $a_{FeS} = 1$ for stoichiometric FeS, with negligible uncertainty). The uncertainties in the S contents of the silicate glass were taken to be the observed uncertainty in S content as given in Table 2, plus 60 ppm, the limit of detection of S in our electron microprobe analyses. The need to increase the uncertainty in the S contents in this way is based on the observed scatter in the data from duplicate runs (Tables 1 and 2). Some of this scatter may be due to changes in the major element composition of the silicate melt (mainly addition or subtraction of FeO by interaction with the capsule, Table 1).

The results of the fitting procedure are summarized in Table 3. We found that a statistically satisfactory fit of the data required different values of the A and B parameters (i.e., the entropy and enthalpy terms) for the basaltic and the picritic compositions. The need for different values for different compositions is expected from the data for metallurgical slag compositions. The data for both picritic and basaltic melt compositions can be fitted to the same value of the C parameter (the pressure-dependence term). The overall value of the reduced chi-squared (χ^2_ν) for both compositions, fitted simultaneously, is 1.43, indicating that the model fits the data well within the estimated experimental uncertainties.

We emphasize that by including the correction for a_{FeS} for the experiments done in Fe capsules, we are able to fit both these experiments ($a_{FeS} < 1$), and those in FeIr capsules ($a_{FeS} = 1$), to the same equation. Our results therefore support the theoretical expectation (Eqn. 8) that the value of SCSS should be independent of fO_2 and fS_2 under conditions where sulfate is unimportant.

Table 3. Results of non-linear least squares regression analyses of sulfur contents at sulfide saturation (SCSS) of various silicate melt compositions, fitted to Eqn. 10.

		Parameters			
Silicate melt	Number	A	B	C	χ^2
This study					
Synthetic basalt	23	−6684 (597)	11.52 (0.34)	−0.047 (0.004)	1.51
Synthetic picrite	5	+683 (1934)	7.97 (1.07)	[−0.047]	0.37
Wendlandt (1982)					
Grand Ronde	6	−9283 (2024)	13.42 (1.18)	−0.053 (0.012)	0.34
Basalt		−9555 (1976)	13.49 (1.17)	[−0.047]*	0.40
Goose Island	6	−8438 (1934)	13.10 (1.16)	−0.035 (0.009)	0.04
Basalt		−8393 (1959)	13.18 (1.17)	[−0.047]*	0.27
Mt. Hood	6	−18315 (5058)	18.79 (2.98)	−0.099 (0.023)	0.01
Andesite		−18702 (4924)	18.43 (2.90)	[−0.047]*	1.53

*Value of C fixed at −0.047 (see text).

3. DISCUSSION

The present results basically confirm the findings of Wendlandt (1982) that SCSS decreases markedly with pressure. Here we have shown theoretically that the form of this decrease is exponential (Eqn. 8), and empirically that our experimental data fit well to an equation of this form (Fig. 2 and 3). The resultant P-T-S surface (Fig. 4) clearly demonstrates that, over the range 1200–1800°C, and 0–100 kb, SCSS varies 3 orders of magnitude as a function of pressure, but only one order of magnitude as a function of temperature.

We have also fitted the experimental data of Wendlandt (1982) to this equation. These data consist of six experiments each on three compositions, over the pressure range 12–30 kb, the temperature range 1300–1460°C, at an oxygen fugacity presumably defined by the graphite-vapor equilibrium in the C-O-S system. The results of the regression analyses are also given in Table 3. Each set of data was fitted in two ways, firstly allowing the C parameter to vary, and secondly by fixing the C parameter at the value of -0.047 K bar^{-1} found for the synthetic basalt and picrite compositions used in this work. For the two basaltic compositions used by Wendlandt (Grande Ronde and Goose Island basalt) the C parameters returned by the unconstrained regressions are within one combined standard deviation of this value. The Mt. Hood andesite composition yields a somewhat larger value of the C parameter (indicating a greater decrease of SCSS with pressure), but the quoted uncertainties in the data are such that a reasonable fit can still be achieved assuming our value of the C parameter ($\chi^2_\nu = 1.53$ in this case). The reason for the unrealistically low values of χ^2_ν found for the other regressions of the Wendlandt data (indicating that the quoted uncertainties are too large) is not known.

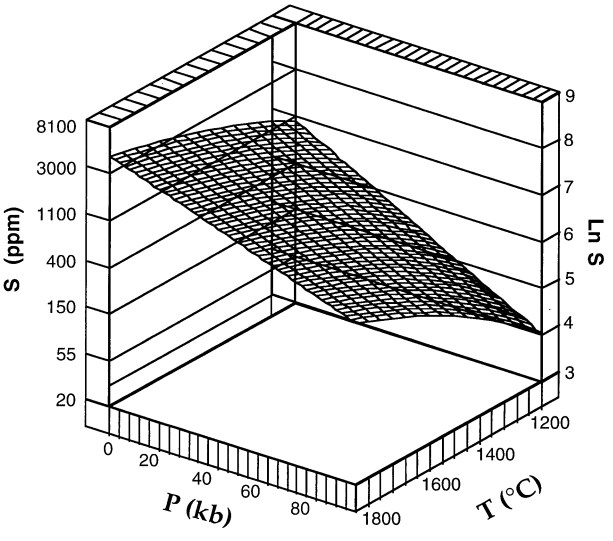

Fig. 4. SCSS in synthetic basalt vs. pressure and temperature (from Eqn. 10 using basalt parameters from Table 3).

Wendlandt (1982) used the graphite-CO_2 buffer to control fO_2, and therefore all his experiments are saturated in CO_2 (i.e., $pCO_2 = p_{total}$). According to Pan et al. (1991), the solubility of CO_2 in a basaltic (tholeiitic) melt under such conditions should increase from ~0.8 wt% at 12 kb to >2.5 wt% at 30 kb. The similarity in the pressure dependence of SCSS from our results and those of Wendlandt therefore implies that CO_2 has little effect on the SCSS of basaltic melts.

The pressure dependence of the SCSS at 2000°C of a rather unusual composition, the Allende CV3 carbonaceous chondrite less some Fe, can also be estimated from the recent experimental data of Li and Agee (1996). This set of data consists of six experimental runs over the pressure range 25–200 kb. Regression of the data to the simplified, constant-temperature, form of Eqn. 10, with data weighted according to reported uncertainties, gives:

$$\ln [S/ppm]_{SCSS} = 8.29(\pm 0.10) - 0.019\ (\pm 0.002)P/T$$

with $\chi^2_\nu = 11.9$. The relatively poor fit may reflect the compositional variability of the silicate melts in these experiments, caused by different degrees of Fe loss. Nevertheless, the experiments of Li and Agee (1996) show a value of the C parameter of the same sign and of fairly similar magnitude to that found for our experiments, and for those of Wendlandt (1982).

In contrast to the effect of pressure, the effect of temperature on SCSS is relatively small. The small magnitude of the temperature effect is confirmed by the high temperature experiments of Li and Agee (1996). Consequently, during adiabatic

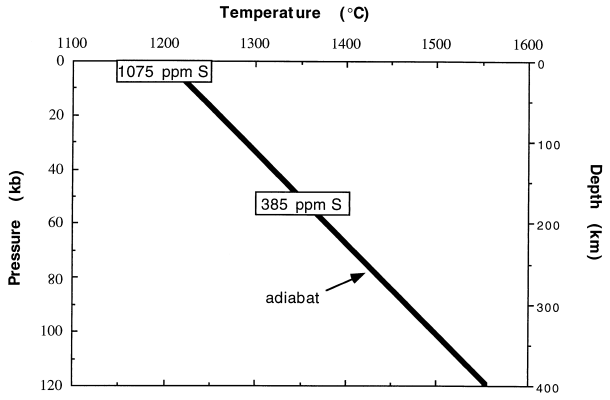

Fig. 5. Calculated SCSS along an adiabatic uplift path of 3°C/kb (derived from Fig. 4).

uprising of a melt, the decrease in pressure outweighs the decrease in temperature, and a melt will arrive at the surface undersaturated in S, even if it were sulfur saturated at its source.

As a quantitative example, we consider a melt of similar composition (i.e., having similar Cs and a_{FeO}) to our experimental basalt, with a potential eruption temperature of 1200°C. From Eqn. 10, this basalt would, if generated at 50 kb (hence 1350°C) contain 385 ppm S, at sulfide saturation (because the primitive mantle abundance of S is ~200 ppm, and the degree of partial melting seldom exceeds 40%, sulfur saturation at source seems likely for all except the very highest degree mantle melts known, the peridotitic komatiites, and melts generated from already depleted sources, such as boninites). As the magma ascends, the amount of dissolved S that would be needed to maintain sulfide saturation steadily increases, reaching 1075 ppm S at zero pressure (i.e., at the Earth's surface). This is illustrated in Fig. 5. Hence the melt would be undersaturated by 690 ppm S, and would require 60% crystallization (e.g., of olivine for a primitive picritic melt) to return to sulfide saturation (this calculation ignores the effect that crystallization would have on melt composition, hence C_S and a_{FeO}). This would not seem to be a realistic mechanism for the production of economically important magmatic sulfide deposits, however, because such extensive fractional crystallization would strip the melt of Ni before sulfide saturation occurred, resulting in a Ni-poor immiscible sulfide.

From the results of this study, we can unequivocally state that unless a mafic melt has either undergone extensive low-pressure fractionation, or has been able to assimilate S, it cannot arrive at the surface S saturated. At $fO_2 \leq$ QFM, oxidation-reduction effects cannot bring on sulfide saturation, because, as we have argued theoretically, and demonstrated experimentally, SCSS is insensitive to fO_2 (apart from its effect on a_{FeS}). Nor will sulfide saturation occur from decreased S solubility due to adiabatic cooling, as influence of temperature on SCSS along a melt adiabat (3°C/kb) is overwhelmed by the effect of decreasing pressure. For high-degree melts such as peridotitic komatiites, that may have completely melted the sulfide phase in their mantle source region, the degree of sulfide undersaturation on eruption will be even more severe. For such melts, which furthermore do not show evidence of having suffered significant fractional crystallization, the necessity of crustal contamination to achieve sulfide saturation, and hence deposition of magmatic sulfide ores, seems essential.

Acknowledgements—We would like to thank WMC for financial support, Dave Green, John Simmonds and Jon Hronsky for the initial conception of, and continued support of this work, Bill Hibberson and Paul Willis for their experimental assistance, and Bob Waterford and Valter Baek Hansen for assistance in developing the Fe-Ir alloy capsules. Discussions with Bob Loucks, and suggestions made by two anonymous reviewers and Tony Naldrett greatly improved the manuscript.

REFERENCES

Brett R. and Bell P. M. (1969) Melting relations in the Fe-rich portion of the system Fe-FeS at 30 kb pressure. *Earth Planet. Sci. Lett.* **6,** 479–482.

Carroll M. R. and Rutherford M. J. (1985) Sulfide and sulfate saturation in hydrous silicate melts. *Proc. Lunar Planet. Sci. Conf.* **15,** C601–C612.

Chuang Y. Y., Hsieh K. C., and Chang Y. A. (1985) Thermodynamics and phase relations of transition metal-sulfur systems: Part V. A reevaluation of the Fe-S system using an associated solution model for the liquid phase. *Met. Trans.* **16B,** 277–285.

Fincham C. J. B. and Richardson F. D. (1954) The behavior of sulphur in silicate and aluminate melts. *Proc. R. Soc. London* **223A,** 40–61.

Haughton D., Roedder P. L., and Skinner B. J. (1974) Solubility of sulphur in mafic magmas. *Econ. Geol.* **69,** 451–467.

Holzheid A., Palme, H., and Chakraborty S. (1997) The activities of NiO, CoO and FeO in silicate melts. *Chem. Geol.*. **139,** 21–38.

Kaiura G. H. and Toguri J. M. (1979) Densities of the molten FeS, Cu_2S and Fe-S-O systems-utilizing a bottom-balance Archimedean technique. *Can. Met. Quart.* **18,** 155–164.

Kongoli F., Dessureault Y., and Pelton, A. D. (1998) Thermodynamic modeling of liquid Fe-Ni-Cu-Co-S mattes. *Met. Trans.* (in press).

Kress V. (1997) Thermochemistry of sulfide liquids. 1. The system O-S-Fe at 1 bar. *Contrib. Min. Pet.* **127,** 176–186.

Li J. and Agee C. B. (1996) Geochemistry of mantle-core differentiation at high pressure. *Nature* **381,** 686–689.

Lorand J. P. (1990) Are spinel lherzolite xenoliths representative of the abundance of sulfur in the mantle? *Geochim. Cosmochim. Acta* **54,** 1487–1492.

Luhr J. F. (1990) Experimental phase relations of water- and sulphur-saturated arc magmas and the l982 eruptions of El Chichon volcano. *J. Petrol.* **31,** 1071–1114.

Mysen B. O. and Popp R. K. (1980) Solubility of sulphur in $CaMgSi_20_6$ and $NaAlSi_30_8$ melts at high pressure and temperature with controlled $f(0_2)$ and $f(S_2)$. *Amer. J. Sci.* **280,** 788–792.

Naldrett A. J. (1989) *Magmatic Sulfide Deposits*. Clarendon Press.

Ohtani E. and Ringwood A. E. (1984) Composition of the core, I. Solubility of molten iron at high temperatures. *Earth Planet. Sci. Lett.* **71,** 85–93.

O'Neill H. St.C. (1991) The origin of the moon and the early history of the Earth—A chemical model. Part 2: The Earth. *Geochim. Cosmochim. Acta* **55,** 1159–1172.

O'Neill H. St.C. and Mavrogenes J. A. (1998) The use of Fe-Ir alloy capsules as fO_2 buffers in experimental petrology. *Amer. Mineral.* (submitted).

O'Neill H. St.C. and Wall V. (1987) The olivine-orthopyroxene-spinel oxygen geobarometer, the Ni precipitation curve, and the oxygen fugacity of the Earth's upper mantle. *J Petrol.* **28,** 1169–1191.

Pan V., Holloway J. R. and Hervig R. L. (1991) The temperature and pressure dependence of carbon dioxide solubility in tholeitic basalt melts. *Geochim. Cosmochim. Acta* **55,** 1587–1595.

Ringwood A. E. and Hibberson W. O. (1990) The system Fe-FeO revisited. *Phys. Chem. Minerals* **17,** 313–319.

Shima H. and Naldrett A. J. (1975) Solubility of sulfur in an ultramafic melt and the relevance of the system Fe-S-O. *Econ. Geol.*. **68,** 79–96.

Sosinsky D. J. and Sommerville I. D. (1986) The composition and

temperature dependence of the sulfide capacity of metallurgical slags. *Met. Trans. B* **16B,** 331–337.

Usselman T. M. (1975) Experimental approach to the state of the core: Part 1. The liquidus relations of the Fe-rich portion of the Fe-Ni-S system from 30 to 100 kb. *Amer. J. Sci.* **275,** 278–290.

Watson E. B. (1994) Diffusion in volatile-bearing magmas. In Volatiles in Magmas (ed. M. R. Carroll and J. R. Holloway); Rev. Mineral. 30, 371–411.

Wallace P. and Carmichael I. S. E. (1992) Sulfur in basaltic melts. *Geochim. Cosmochim. Acta* **56,** 1863–1874.

Wendlandt R. F. (1982) Sulfide saturation of basalt and andesite melts at high pressures and temperatures. *Amer. Mineral.* **67,** 877–885.

Woodland A. B. and O'Neill, H. St.C. (1997) Thermodynamic data for Fe-bearing phases obtained using noble metal alloys as redox sensors. *Geochim. Cosmochim. Acta* **61,** 4359–4366.

Young R. W., Duffy J. A., Hassall G. J., and Xu Z. (1992) Use of optical basicity concept for determining phosphorus and sulphur slag-metal partitions. *Ironmaking and Steelmaking* **19,** 201–219.